A thieno[3,2-c]pyridine-4,6-dione derived bisisoindigo for organic field-effect transistors

Chang Li[†], Fangliang Dong[†], Rui Ge[†], Ming Wang[†*]

[†]State Key Laboratory for Modification of Chemical Fibers and Polymer Materials, Center for Advanced Low-dimension Materials, College of Materials Science and Engineering, Donghua University, Shanghai, 201620, China

KEYWORDS. conjugated polymers, isoindigo, organic field-effect transistors, ambipolar, charge carrier mobility.

E-mail: mwang@dhu.edu.cn

Supplementary Information

Content

1. General methods

UV-Vis-NIR absorption spectra were recorded on a Perkin Elmer Lambda 950 spectrophotometer. Nuclear magnetic resonance (NMR) spectra were obtained on a Bruker 400 MHz spectrometer. High temperature gel permeation chromatography (HT-GPC) was performed on an Agilent PL-GPC 220 System using the eluent of chlorobenzene at 80 °C, and molecular weights were calculated relative to linear PS standards. Geometry and orbital calculations of polymers were carried out based on the density functional theory (DFT) CAM-B3LYP together with 6-31G(d,p) basis set by using the Gaussian 16 package on Swordfish-Cluster at the Shanghai Supercomputer Center. Thermogravimetric analysis (TGA) was performed on a TA instrument (TA Discovery TGA550) with about 1 ~ 3 mg polymers samples at a rate of 10 °C / min. Differential scanning calorimetry (DSC) measurements were carried out on a Discovery DSC250 instrument with about 1 ~ 3 mg polymer samples at a rate of 5 °C / min under nitrogen atmosphere. Cyclic voltammetry (CV) measurements were tested on a CHI-730 electrochemistry workstation. OFET devices were measured in a nitrogen atmosphere glovebox using a PRCBE SZ-6 probe station and a Keithley 4200A-SCS parameter analyzer. GIWAXS samples were prepared on Si substrates. The 10 keV X-ray beam was incident at a grazing angle of 0.11°-0.15°, which maximized the scattering intensity from the samples. In-plane and out-of-plane sector averages were calculated using the Nika software package. Tapping-mode atomic force microscopy (AFM) images were recorded by a Bruker Dimension Icon.

2. Synthetic procedure

4*H*-thieno[3,2-*c*]pyran-4,6(7*H*)-dione (**1**),[1] 5-(2-octyldodecyl)thieno[3,2-c]pyridin e-4,6(5*H*,7*H*)-dione (**2b**),[1] 3,8-dihydroindolo[7,6-*g*]indole-1,2,6,7-tetraone (**3**),[2] 3,8-didodecyl-3,8-dihydroindolo[7,6-*g*]indole-1,2,6,7-tetraone (**4b**)[2] and 5,5'-bis(trimeth ylstannyl)-2,2'-bithiophene (**6**)[3] were synthesized according to reported methods. Other regents were purchased from commercial resources. All solvents for react ions were purified and dried before use.

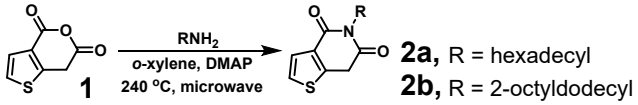

*5-hexadecylthieno[3,2-c]pyridine-4,6(5H,7H)-dione (**2a**)*: In a nitrogen atmosphere glovebox, compound **1** (800 mg, 4.8 mmol, 1.0 eq.), DMAP (146 mg, 1.2 mmol, 0.25 eq.) and *o*-xylene (12 mL) were charged into a 20 mL microwave tube, then 1-hexadecylamine (1159 mg, 4.8 mmol, 1.0 eq.) was added into the mixture under stirring in 15 minutes. The tube was sealed and then heated at 240 ℃ for 2 hours through a microwave initiator. Then the *o*-xylene was removed via rotavapor and the crude product was purified via silica-gel chromatograph using mineral ether and dichloromethane (1:3, v/v) as the eluent to produce the pure product as dark red oil (0.65 g, 1.66 mmol, 35% yield). ^{1}H NMR (chloroform-*d*, 298 K, 400 MHz, δ/ppm): 7.5 (d, 1H), 7.28 (d, 1H), 4.11 (s, 2H), 3.94-3.90 (m, 2H),1.62-1.55 (m, 2H), 1.36-1.24 (m, 26H), 0.88 (t, 3H). ^{13}C NMR (chloroform-*d*, 298 K, 100 MHz, δ/ppm): 168.34, 160.95, 143.02, 139.88, 125.86, 125.21,40.03, 34.25, 31.95, 29.72, 29.69, 29.67, 29.65, 29.62, 29.59, 29.56, 29.55 29.38, 29.35, 28.04, 27.05, 22.72, 14.15.

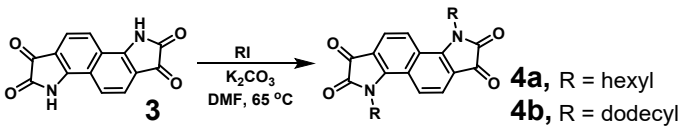

*3,8-dihexyl-3,8-dihydroindolo[7,6-g]indole-1,2,6,7-tetraone (**4a**)*: To a suspension of **3** (1.0 g, 3.76 mmol, 1.0 eq.) in anhydrous DMF (15.0 mL) was added freshly dried K_2CO_3 (2.1 g, 15.03 mmol, 4.0 eq.). The mixture was heated to 65 ℃. After 1 hour, 1-iodohexane (2.39 g, 11.27 mmol, 3.0 eq.) was added in one portion. The reaction

mixture was stirred at 65 °C. for 6 hours. The reaction mixture was cooled down to room temperature and poured over water and acidified with 1M HCl to pH of 7. The aqueous layer was extracted with dichloromethane, washed with water, brine and dried over $MgSO_4$. The solvent was removed under vacuum. The crude product was purified by silica-gel column chromatography using dichloromethane and ethyl acetate (1/4, v/v) as the eluent, washed with hexane and filtered. The final product was obtained as blue solid (244 mg, 0.56 mmol, 15%). ^{1}H NMR (chloroform-*d*, 298 K, 400 MHz, δ/ppm): 7.96 (d, 2H), 7.68 (d, 2H), 4.24 (t, 4H), 1.87-1.77 (m, 4H), 1.5-1.25 (m, 12H), 0.89 (t, 28Hz, 6H). ^{13}C NMR (chloroform-d, 298 K, 100 MHz, δ/ppm): 182.85, 159.03, 152.22, 127.30, 120.28, 119.64, 116.22, 43.52, 31.30, 29.71, 29.27, 26.33, 22.49, 13.96.

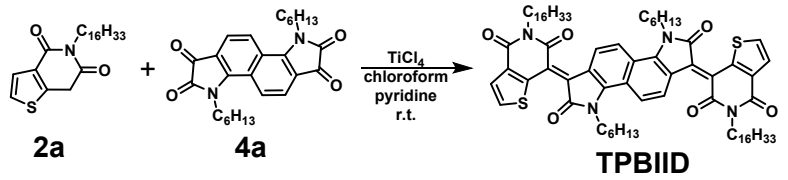

(7Z,7'Z)-7,7'-(3,8-dihexyl-2,7-dioxo-2,3,7,8-tetrahydroindolo[7,6-g]indole-1,6-diylidene)bis(5-hexadecylthieno[3,2-c]pyridine-4,6(5H,7H)-dione) (***TPBIID***): Compound **2a** (0.397 g, 1.012 mmol) and **4a** (0.200 g, 0.460 mmol) were dissolved in chloroform (10.0 mL) in a round-bottom flask (50 mL). Then titanium tetrachloride (0.1 mL) and pyridine (0.1 mL) were also added to the flask. The reaction mixture was stirred at 60 °C for 1 hour under nitrogen. The reaction was cooled to room temperature and quenched in water. Then the crude product was extracted with dichloromethane. The organic phase was dried over $MgSO_4$, evaporated to remove the solvent, and purified by silica-gel column chromatography using mineral ether and dichloromethane (1/3, v/v) as the eluent to obtain the pure product as green solid (217.4 mg, 40%). ^{1}H NMR (chloroform-*d*, 298 K, 400 MHz, δ/ppm): 7.82 (d, 2H), 7.74-7.70 (m, 4H), 7.54 (d, 2H), 4.28 (t, 4H), 4.13 (t, 4H), 1.93-1.70 (m, 8H), 1.52-1.17 (m, 64H), 0.97-0.81 (m, 12H). ^{13}C NMR (chloroform-*d*, 298 K, 100 MHz, δ/ppm): 167.1, 163.88, 158.45, 141.73, 138.11, 131.95, 130.46, 130.19, 127.68, 125.64, 121.59, 121.16, 118.87,

115.48, 41.87, 39.73, 30.39, 30.39, 29.86, 29.86, 28.17, 28.16, 28.15, 28.13, 28.09, 28.06, 27.89, 27.86, 27.83, 26.84, 25.63, 24.96, 21.16, 21.04, 12.60, 12.49.

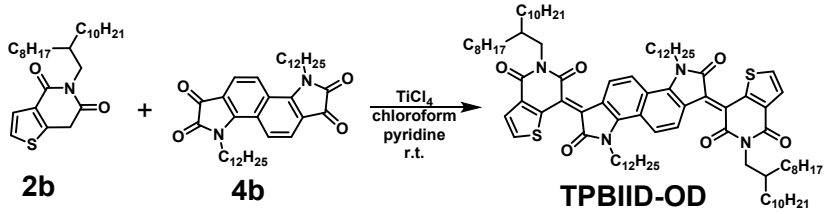

(7Z,7'Z)-7,7'-(3,8-didodecyl-2,7-dioxo-2,3,7,8- tetrahydroindolo[7,6-g]indole-1,6-diylidene)bis(5-(2-octyldodecyl)thieno[3,2-c]pyridine-4,6(5H,7H)-dione) ***(TPBIID-OD)***: Compound **2b** (0.397 g, 0.829 mmol) and **4b** (0.200 g, 0.332 mmol) were dissolved in chloroform (10.0 mL) in a round-bottom flask (50 mL). Then titanium tetrachloride (0.1 mL) and pyridine (0.1 mL) were also added to the flask. The reaction mixture was stirred at 60 °C for 1 hour under nitrogen. The reaction was cooled to room temperature and quenched in water. Then the crude product was extracted with dichloromethane. The organic phase was dried over $MgSO_4$, evaporated to remove the solvent, and purified by silica-gel column chromatography using mineral ether and dichloromethane (1/2, v/v) as the eluent to obtain the pure product as green solid (169.7 mg, 35%). ^{1}H NMR (chloroform-*d*, 298 K, 400 MHz, δ/ppm): 7.84 (d, 2H), 7.74-7.70 (m, 4H), 7.54 (d, 2H), 4.28 (t, 4H), 4.07 (t, 4H), 2.04-1.94 (m, 2H), 1.92-1.82 (m, 4H), 1.40-1.15 (m, 100H), 0.88-0.83 (m, 18H). ^{13}C NMR (chloroform-*d*, 298 K, 100 MHz, δ/ppm): 166.20, 163.33, 157.95, 140.69, 137.09, 131.04, 129.55, 129.07, 126.97, 124.78, 120.66, 120.15, 117.89, 114.52, 42.75, 40.95, 34.43, 29.46, 29.44, 29.42, 29.40, 29.38, 27.59, 27.21, 27.20, 27.19, 27.18, 27.17, 27.16, 27.15, 27.14, 27.13, 27.12, 26.95, 26.91, 26.88, 26.87, 26.85, 24.45, 24.14, 20.23, 20.22, 20.20, 11.65, 11.64, 11.63.

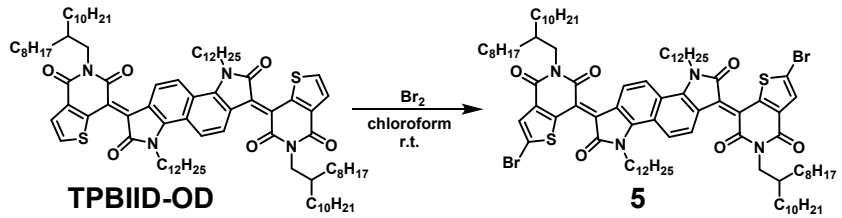

(7Z,7'Z)-7,7'-(3,8-didodecyl-2,7-dioxo-2,3,7,8-tetrahydroindolo[7,6-g]indole-1,6-diylidene)bis(2-bromo-5-(2-octyldodecyl)thieno[3,2-c]pyridine-4,6(5H,7H)-dione) (***5***): The bromine (35 mg, 0.218 mmol) was dissolved in 2 mL of chloroform and then was added dropwise into a solution of **TPBIID-OD** (160 mg, 0.109 mmol) in 5 mL chloroform at 0 °C. Then the reaction was warmed to room temperature and stirred for 2 hours. The reaction was quenched in 50 mL water, and the organic layer was extracted with chloroform for three times. The chloroform fractions were combined and dried over $MgSO_4$, then the organic solvent was removed under a reduced pressure via a rotavapor. The residue was further purified by silica-gel column chromatography using dichloromethane and mineral ether (2/1, v/v) as the eluent. The compound **5** was obtained as green solid (141 mg, yield 80%). ^{1}H NMR (chloroform-*d*, 298 K, 400 MHz, δ/ppm): 7.81 (d, 2H), 7.72-7.68 (m, 4H), 4.28 (t, 4H), 4.05 (t, 4H), 2.04-1.94 (m, 2H), 1.92-1.82 (m, 4H), 1.49-1.17 (m, 100H), 0.91-0.80 (m, 18H). ^{13}C NMR (chloroform-*d*, 298 K, 100 MHz, δ/ppm): 166.38, 162.73, 156.81, 140.75, 137.97, 130.95, 128.57, 127.16, 125.96, 120.69, 120.18, 119.65, 117.78, 114.62, 42.75, 40.95, 34.43, 29.46, 29.44, 29.42, 29.40, 29.38, 27.59, 27.21, 27.20, 27.19, 27.18, 27.17, 27.16, 27.15, 27.14, 27.13, 27.12, 26.95, 26.91, 26.88, 26.87, 26.85, 24.45, 24.14, 20.23, 20.22, 20.20, 11.65, 11.64, 11.63.

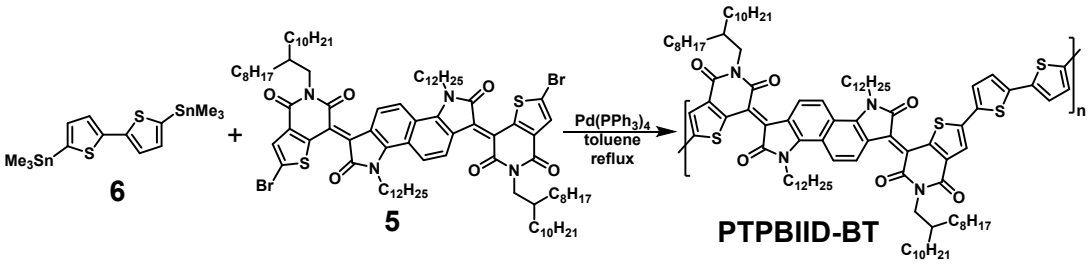

PTPBIID-BT: In a dry 0.5-2 mL microwave reaction vial, monomer **5** (0.1 g, 0.0617 mmol), **6** (31.2 mg, 0.0635 mmol), $Pd(PPh_3)_4$ (3.56 mg, 0.003 mmol) and toluene (1.5 mL) were added inside a nitrogen atmosphere glovebox. The vial was then sealed using a Teflon®cap and put in oil bath to heat to reflux with stirring for 9 hours. The reaction was allowed to cool to room temperature. The vail was then transferred to the glovebox to add $Pd(PPh_3)_4$ (3 mg), 2-bromothiophene (0.1 mL) and toluene (0.5 mL) for end-

capping reaction in oil bath to heat to reflux with stirring for an hour. The reaction was allowed to cool to room temperature and the polymer was precipitated in methanol. The precipitates were collected by filter paper and extracted with methanol, hexane, dichloromethane, chloroform and chlorobenzene via a Soxhlet extractor, respectively. The chlorobenzene fraction was concentrated via a rotavapor and then passed through a short silica-gel (60-100 mesh) column. The collected polymer solution was concentrated again and was drop-wised to methanol under stirring. The polymer was precipitated and collected via a filter paper, dried over in the vacuum to obtain the final product as black solid (50mg, yield 49%). Molecular weight (in chlorobenzene at 80 °C): M_n = 45.6 kDa, PDI = 3.0

Reference

1. F.-L. Dong, Y. Zhang, H. Wei, C. Li, Z. Li, J. Gao, Y. Hu, Z. Tang, and M. Wang, *ACS Appl. Polym. Mater.*, 2023, **5**, 9056–9062.

2. K. Huang, X. Zhao, Y. Du, S. Kim, X. Wang, H. Lu, K. Cho, G. Zhang, and L. Qiu, *J. Mater. Chem. C*, 2019, **7**, 7618–7626.

3. T. Lei, Y. Cao, Y. Fan, C.-J. Liu, S.-C. Yuan, and J. Pei, *J. Am. Chem. Soc.*, 2011, **133**, 6099–6101.

3. Thermal analysis

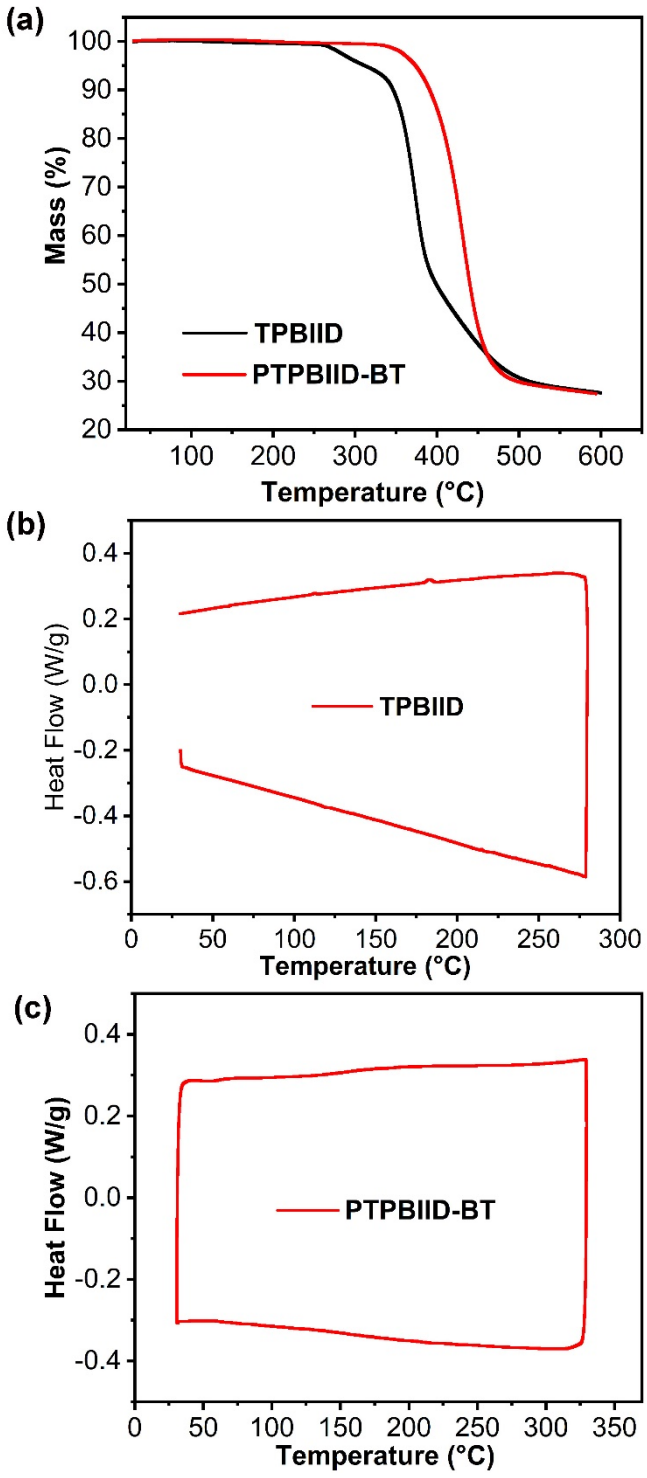

Figure S1. Thermal properties of TPBIID and PTPBIID-BT: (a) TGA measurements of TPBIID and PTPBIID-BT; (b) DSC measurement of TPBIID; (c) DSC measurement of PTPBIID-BT.

4. Quantum chemistry simulation

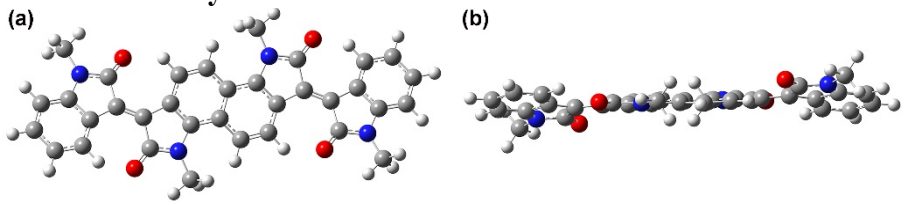

Figure S2. Geometries of bisisoindigo structure: (a) top-view; (b) side-view.

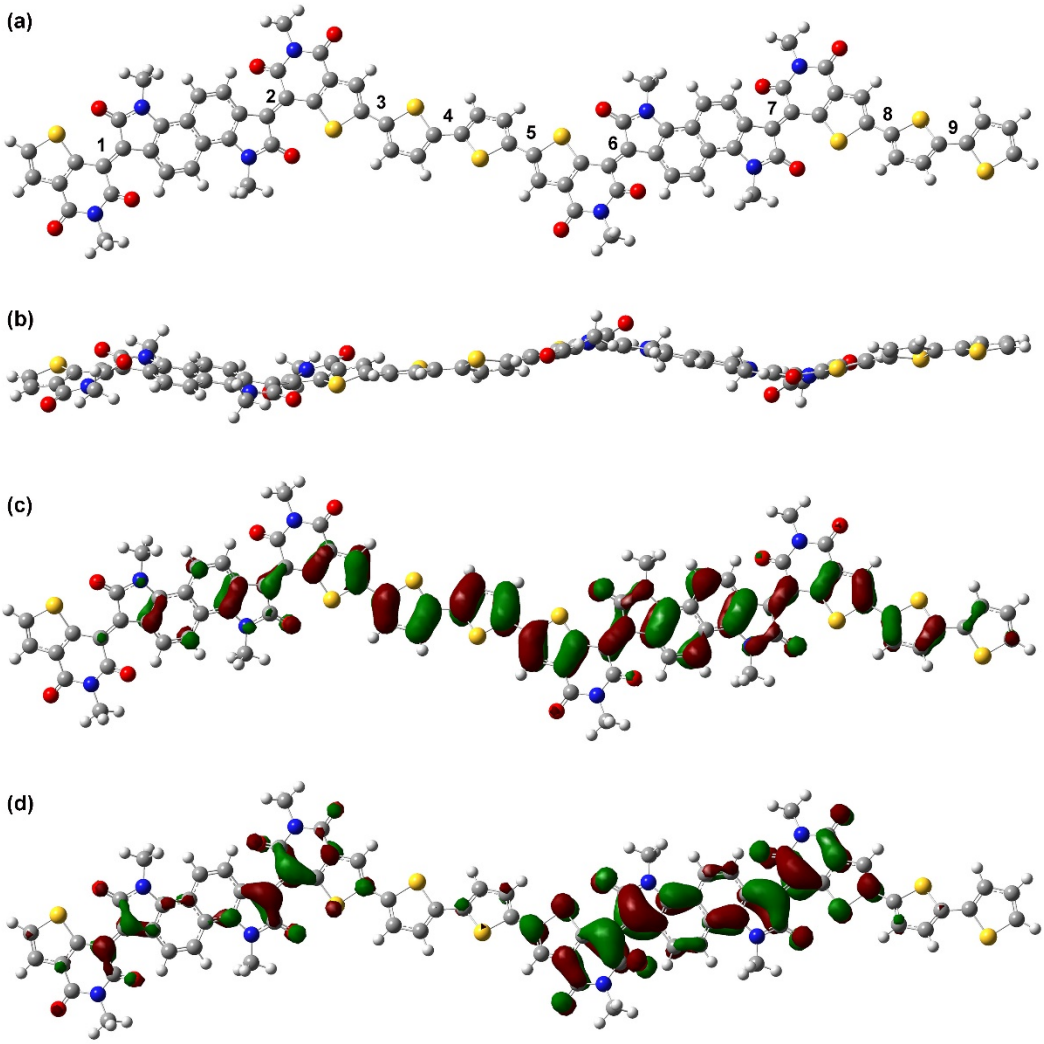

Figure S3. PTPBIID-BT dimer: (a) top-view; (b) side-view; (c) HOMO; (d) LUMO.

Table S1. Dihedral angles of PTPBIID-BT dimer in Figure S3a.

Label	1	2	3	4	5	6	7	8	9	average
Dihedral (°)	18.0	18.6	15.9	18.6	19.5	18.7	18.7	18.8	23.3	18.9

5. Cyclic voltammetry measurements

A three-electrode cell equipped with a glassy carbon working electrode, an Ag/AgCl reference electrode and a Pt wire counter-electrode. The measurements were performed in absolute acetonitrile with tetrabutylammonium hexafluorophosphate (0.1 M) as the supporting electrolyte at a scan rate of 50 mV/s under a nitrogen atmosphere. Semiconductor films for were drop-casted onto the glassy carbon working electrode from their chlorobenzene solution at a concentration of 5 mg/mL. The oxidation-reduction potential of ferrocene was also measured as the reference. The absolute energy level of ferrocene/ferrocenium (Fc/Fc^+) was set to be 4.8 eV below vacuum. The E_{HOMO} and E_{LUMO} were calculated from the equations of "$E_{HOMO} = (E_{ox} - E_{ferrocene} + 4.8)$ eV" and "$E_{LUMO} = -(E_{red} - E_{ferrocene} + 4.8)$ eV", where E_{ox} and E_{red} were the oxidation and reduction onsets, respectively, and $E_{ferrocene}$ is the oxidation-reduction potential.

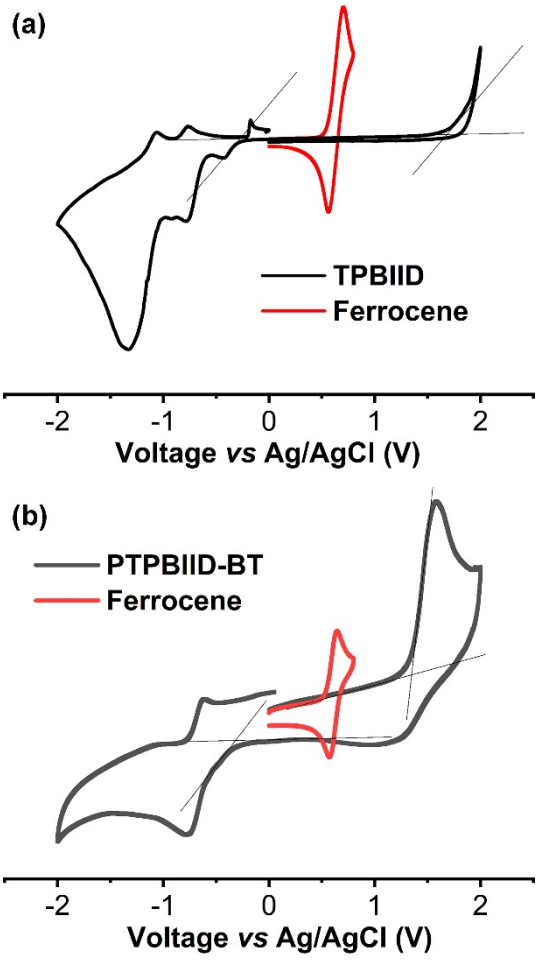

Figure S4. Cyclic voltammetry measurements of: (a) TPBIID; (b) PTPBIID-BT.

6. OFET fabrication and performance

Device fabrication: Substrates with source and drain contacts (Ti/Au, 2/35 nm) were custom-made in First MEMS Co., Ltd. using photolithography process. Before polymer deposition, the substrates were cleaned by sonication in acetone and isopropanol for 3 minutes each, and were then dried in an oven under ambient atmosphere at 120 °C for 10 minutes, treated with UV-O_3 for 15 minutes, and then passivated by using decyltrichlorosilane (from Gelest Chemicals) from a 1 vol% solution in toluene at 120 °C for 2 hours. The substrates were then rinsed and sonicated in toluene and dried under nitrogen flow. TPBIID films were spin-coated from the chloroform solution at a concentration of 5 mg/mL. PTPBIID-BT films were spin-coated from the chlorobenzene solution at a concentration of 5 mg/mL. The final device architecture (from bottom to top) for these bottom gate, bottom contact field-effect transistors was Si/ SiO_2/DTS/ Au/Polymer semiconductor layer. The mobility of OFET devices were obtained by fitting the following equation to the saturation regime transfer characteristics: $I_{DS} = (W/2L)\, C_i\, \mu\, (V_{GS} - V_T)^2$, where W is the channel width (1000 μm), L is the channel length (80 μm), C_i is the gate dielectric layer capacitance per unit area (11 nF/cm^2), V_{GS} is the gate voltage, V_T is the threshold voltage, and I_{DS} is the source-drain current. Devices were measured under nitrogen in a glovebox. Hole mobility values were calculated from a gate voltage range of 0 V to -80 V at a source-drain voltage of -80 V, while electron mobility values were calculated from a gate voltage range of 0 V to 80 V at a source-drain voltage of 80 V.

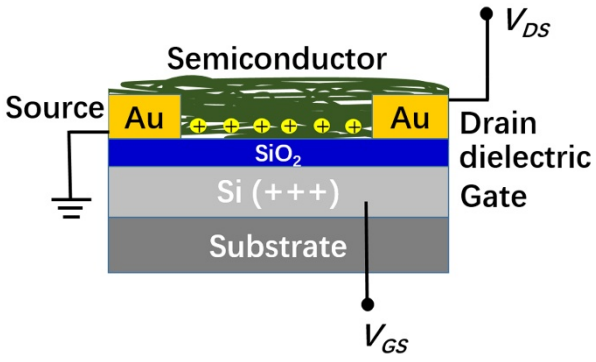

Figure S5. OFET device structure.

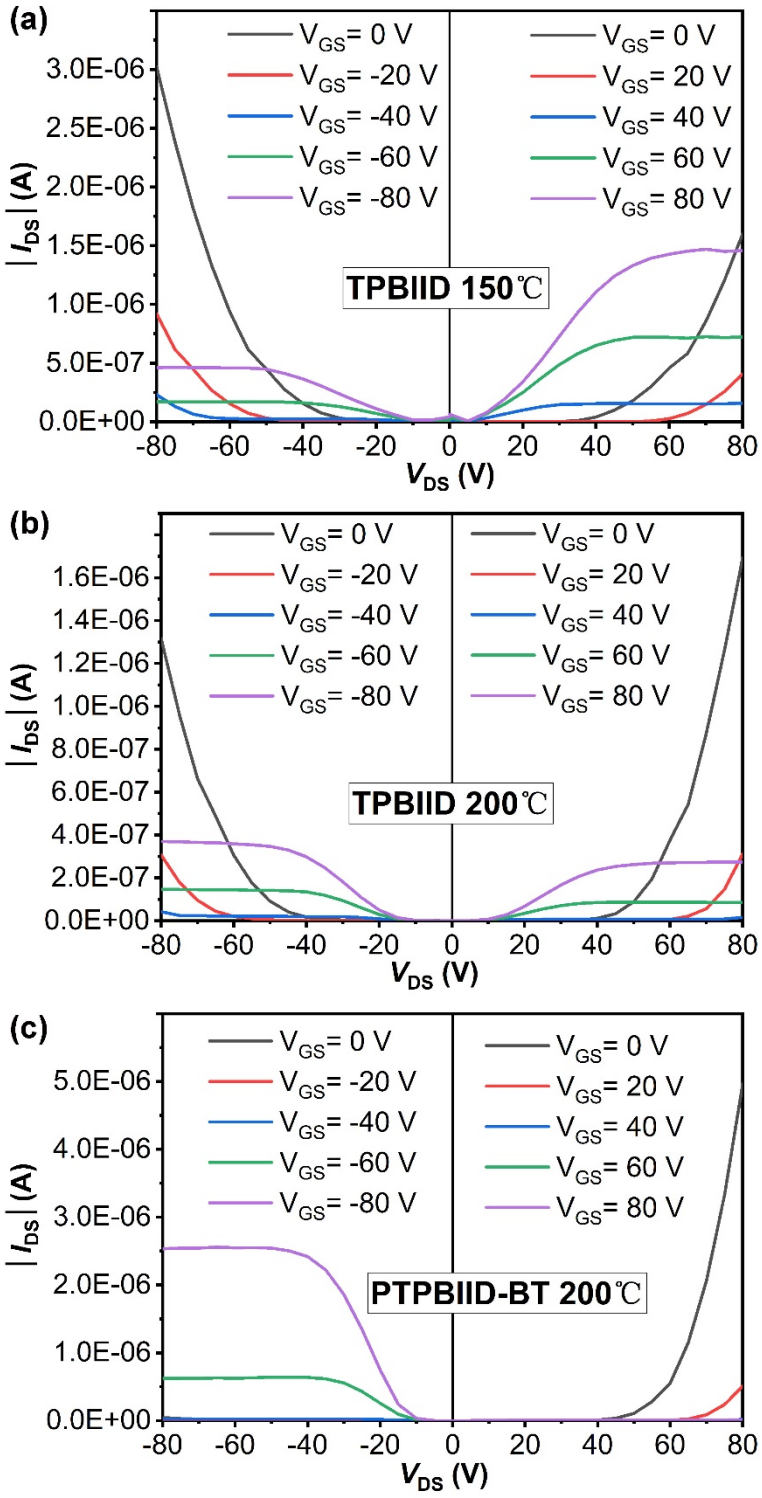

Figure S6. Transfer curves of: (a) TPBIID film annealed at 150 ℃; (b) TPBIID film annealed at 200 ℃; (c) PTPBIID-BT film annealed at 200 ℃.

Table S2. Tested OFET performance of TPBIID devices without annealing.

	p-channel			*n*-channel		
device	Mobility ($cm^2 V^{-1} s^{-1}$)	V_T (V)	On/off	Mobility ($cm^2 V^{-1} s^{-1}$)	V_T (V)	On/off
1	0.00063	-25.46	1.44E+02	0.00147	36.76	5.70E+02
2	0.00118	-42.53	2.59E+05	0.00093	45.44	1.02E+04
3	0.00118	-22.09	1.10E+03	0.00218	37.59	7.56E+03
4	0.00092	-35.00	2.00E+04	0.00126	37.48	7.58E+03
5	0.00110	-15.08	2.95E+02	0.00124	24.61	4.04E+02
6	0.00150	-44.38	8.24E+05	0.00198	43.21	1.23E+04
7	0.00146	-23.34	3.72E+02	0.00246	34.54	2.52E+03
8	0.00077	-38.42	3.70E+04	0.00136	41.62	4.35E+03
9	0.00121	-23.23	9.48E+02	0.00227	37.25	9.16E+03
Average	0.00111	-29.95	1.27E+05	0.00168	37.61	6.07E+03

Table S3. Tested OFET performance of TPBIID devices annealed at 100 ℃.

	p-channel			*n*-channel		
device	Mobility ($cm^2 V^{-1} s^{-1}$)	V_T (V)	On/off	Mobility ($cm^2 V^{-1} s^{-1}$)	V_T (V)	On/off
1	0.00401	-47.91	3.24E+03	0.00093	41.77	8.57E+02
2	0.00273	-32.12	1.38E+02	0.00795	32.57	4.22E+02
3	0.00231	-47.06	1.83E+04	0.00392	43.84	4.75E+03
4	0.00305	-36.32	1.01E+03	0.01125	30.79	9.87E+02
5	0.00379	-43.47	4.28E+03	0.00531	39.55	7.18E+02
6	0.00460	-23.81	7.94E+01	0.01016	20.83	6.30E+01
7	0.00214	-34.00	1.30E+04	0.00727	32.73	3.02E+02
8	0.00207	-48.05	9.24E+01	0.00576	37.69	2.38E+03
9	0.00240	-20.53	9.24E+01	0.00638	42.54	2.28E+03
Average	0.00301	-37.03	4.47E+03	0.00655	35.81	1.42E+03

Table S4. Tested OFET performance of TPBIID devices annealed at 150 ℃.

	p-channel			*n*-channel		
device	Mobility ($cm^2 V^{-1} s^{-1}$)	V_T (V)	On/off	Mobility ($cm^2 V^{-1} s^{-1}$)	V_T (V)	On/off
1	0.00785	-28.40	7.15E+01	0.01472	17.40	5.42E+01
2	0.00584	-35.53	2.87E+02	0.01081	33.63	2.17E+02
3	0.00380	-32.51	2.39E+02	0.01135	23.93	1.88E+02
4	0.00379	-45.76	2.55E+03	0.00594	43.80	1.78E+03
5	0.00416	-35.41	4.29E+02	0.01381	26.86	3.25E+02
6	0.00366	-42.81	2.30E+03	0.01072	36.82	9.09E+02
7	0.00382	-32.22	4.52E+02	0.00642	38.05	7.60E+02
8	0.00317	-43.98	7.65E+02	0.00864	34.14	6.26E+02
9	0.00288	-28.17	3.91E+02	0.01132	25.89	3.01E+02
Average	0.00433	-36.06	8.31E+02	0.01041	31.17	5.74E+02

Table S5. Tested OFET performance of TPBIID devices annealed at 200 ℃.

	p-channel			*n*-channel		
device	Mobility ($cm^2 V^{-1} s^{-1}$)	V_T (V)	On/off	Mobility ($cm^2 V^{-1} s^{-1}$)	V_T (V)	On/off
1	0.00819	-23.27	1.21E+02	0.00979	36.16	1.19E+03
2	0.00785	-28.02	1.21E+02	0.00777	38.67	1.40E+03
3	0.01036	-43.10	1.88E+03	0.00765	35.35	1.12E+03
4	0.00807	-27.90	1.47E+02	0.00913	30.33	3.83E+02
5	0.00904	-43.06	1.64E+03	0.00673	36.57	1.11E+03
6	0.00765	-25.78	1.46E+02	0.00901	34.15	1.33E+03
7	0.01087	-41.46	1.45E+03	0.00728	36.20	1.12E+03
8	0.00781	-32.60	2.11E+02	0.00958	30.15	4.45E+02
9	0.01039	-41.07	1.37E+03	0.00608	34.43	9.00E+02
Average	0.00891	-34.03	7.88E+02	0.00811	34.67	9.99E+02

Table S6. Tested OFET performance of PTPBIID-BT devices without annealing.

	p-channel			*n*-channel		
device	Mobility ($cm^2 V^{-1} s^{-1}$)	V_T (V)	On/off	Mobility ($cm^2 V^{-1} s^{-1}$)	V_T (V)	On/off
1	0.03796	-38.48	7.38E+05	0.00008	53.31	5.88E+05
2	0.02641	-16.78	5.24E+06	0.00004	37.01	1.13E+06
3	0.04504	-43.89	6.38E+05	0.00008	50.90	5.10E+05
4	0.02087	-11.29	1.90E+06	0.00004	35.76	1.36E+06
5	0.04832	-44.97	5.06E+05	0.00007	48.94	3.58E+05
6	0.02382	-21.37	2.70E+06	0.00003	10.29	1.31E+05
7	0.02361	-12.89	8.70E+05	0.00003	33.96	4.71E+05
8	0.04442	-38.11	6.66E+05	0.00009	52.60	2.68E+06
9	0.02528	-11.80	7.30E+04	0.00004	33.25	3.90E+05
Average	0.03286	-26.62	1.48E+06	0.00006	39.56	8.46E+05

Table S7. Tested OFET performance of PTPBIID-BT devices annealed at 100 ℃.

	p-channel			*n*-channel		
device	Mobility ($cm^2 V^{-1} s^{-1}$)	V_T (V)	On/off	Mobility ($cm^2 V^{-1} s^{-1}$)	V_T (V)	On/off
1	0.07247	-49.89	5.48E+05	0.00004	41.00	7.77E+07
2	0.03809	-27.58	6.02E+06	0.00004	5.08	8.07E+04
3	0.06715	-46.31	9.99E+05	0.00005	41.94	3.49E+06
4	0.03702	-27.93	2.57E+06	0.00004	6.29	2.37E+04
5	0.07158	-45.92	7.11E+05	0.00006	43.50	8.36E+06
6	0.07338	-47.37	2.66E+06	0.00006	41.76	3.43E+06
7	0.04792	-20.38	4.38E+06	0.00004	33.73	8.45E+06
8	0.07925	-46.37	2.66E+06	0.00007	46.11	9.45E+05
9	0.04603	-20.66	1.31E+07	0.00005	31.03	2.60E+06
Average	0.05921	-36.94	3.74E+06	0.00005	32.27	1.17E+07

Table S8. Tested OFET performance of PTPBIID-BT devices annealed at 150 °C.

	p-channel			*n*-channel		
device	Mobility ($cm^2 V^{-1} s^{-1}$)	V_T (V)	On/off	Mobility ($cm^2 V^{-1} s^{-1}$)	V_T (V)	On/off
1	0.09536	-37.90	9.44E+05	0.00012	49.97	3.02E+07
2	0.05562	-33.00	1.92E+06	0.00012	19.91	2.71E+04
3	0.09732	-40.10	3.25E+06	0.00011	48.92	5.50E+06
4	0.05618	-33.25	2.20E+06	0.00013	19.92	2.57E+04
5	0.08092	-58.29	3.07E+05	0.00014	42.11	7.82E+06
6	0.06724	-26.47	8.23E+06	0.00012	31.92	8.76E+04
7	0.10594	-41.77	7.26E+06	0.00011	47.05	1.55E+07
8	0.06857	-27.08	3.68E+06	0.00012	32.67	9.26E+04
9	0.10445	-40.68	4.89E+06	0.00011	47.03	1.96E+07
Average	0.08129	-37.62	3.63E+06	0.00012	37.72	8.76E+06

Table S9. Tested OFET performance of PTPBIID-BT devices annealed at 200°C.

	p-channel			*n*-channel		
device	Mobility ($cm^2 V^{-1} s^{-1}$)	V_T (V)	On/off	Mobility ($cm^2 V^{-1} s^{-1}$)	V_T (V)	On/off
1	0.14289	-53.43	8.54E+05	0.00026	45.83	4.44E+05
2	0.09136	-29.53	2.30E+04	0.00025	39.65	1.10E+05
3	0.10317	-37.61	5.40E+05	0.00028	44.10	8.65E+05
4	0.08205	-27.65	3.88E+04	0.00021	41.52	6.87E+04
5	0.06442	-60.50	1.55E+06	0.00026	41.84	4.64E+05
6	0.15692	-52.73	1.27E+06	0.00019	46.08	2.60E+06
7	0.09226	-30.25	7.27E+04	0.00024	41.29	1.32E+05
8	0.14455	-52.10	1.16E+07	0.00018	46.02	2.69E+06
9	0.09516	-28.70	4.01E+04	0.00024	39.95	1.27E+05
Average	0.10809	-41.39	1.78E+06	0.00023	42.92	8.34E+05

7. UV-vis absorption of TPBIID films.

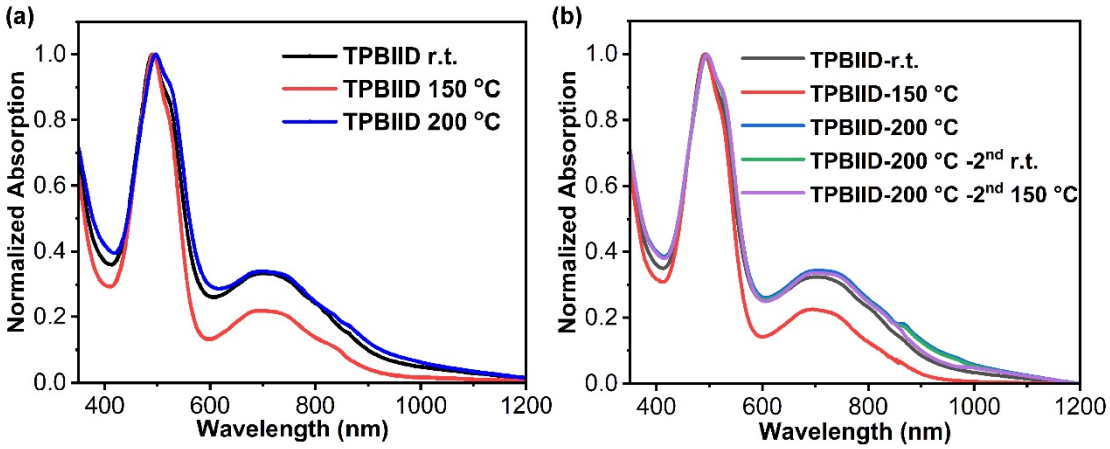

Figure S7. UV-vis absorption of TPBIID films: (a) under different annealing conditions; (b) additional stability test of 200 °C annealing films (2^{nd} means the film was measured after 24 hours of the 1^{st} measurement.).

8. Morphologies of PTPBIID-BT film annealed at 200 °C.

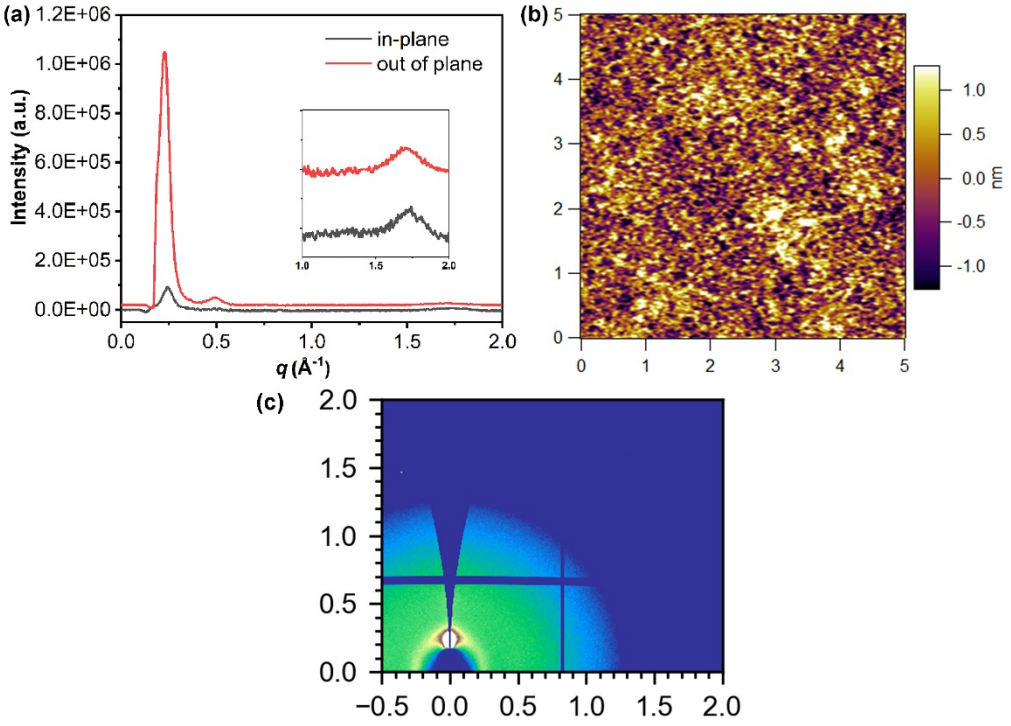

Figure S8. Morphologies of PTPBIID-BT**:** (a) GIWAXS line-cut profile of film annealed at 200 °C; (b) AFM height image of film annealed at 200 °C; (c) GIWAXS 2D image of pristine film.

9. NMR spectra

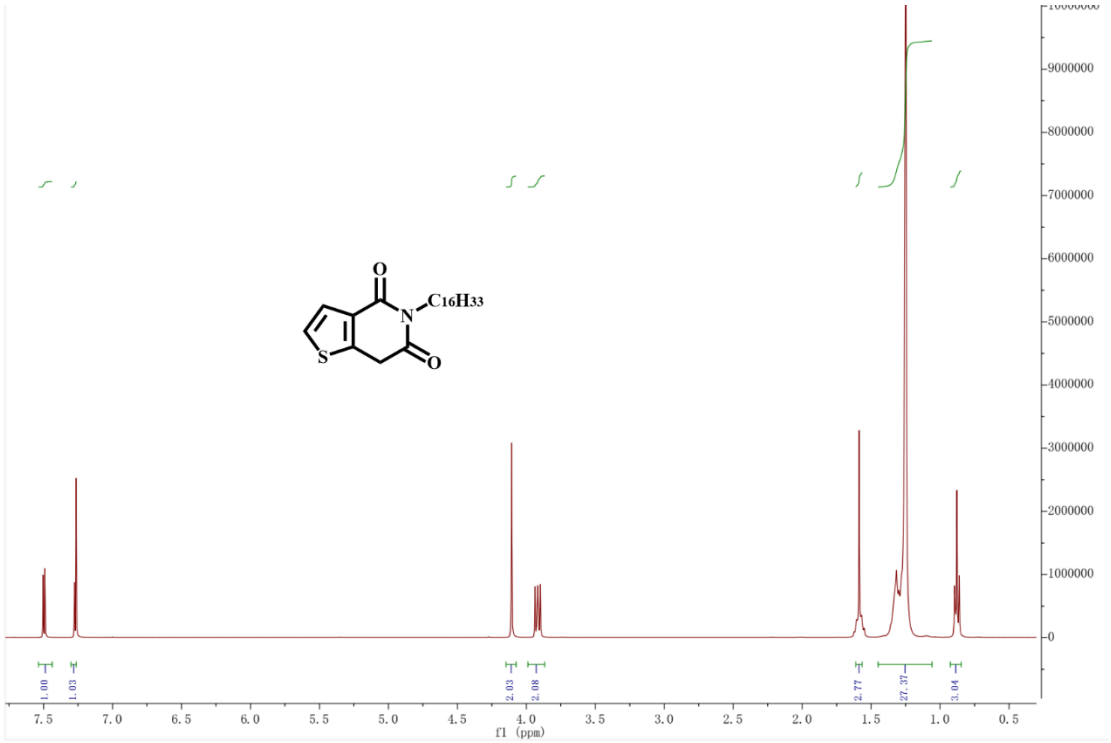

Figure S9. ^{1}H NMR spectrum of compound **2a**.

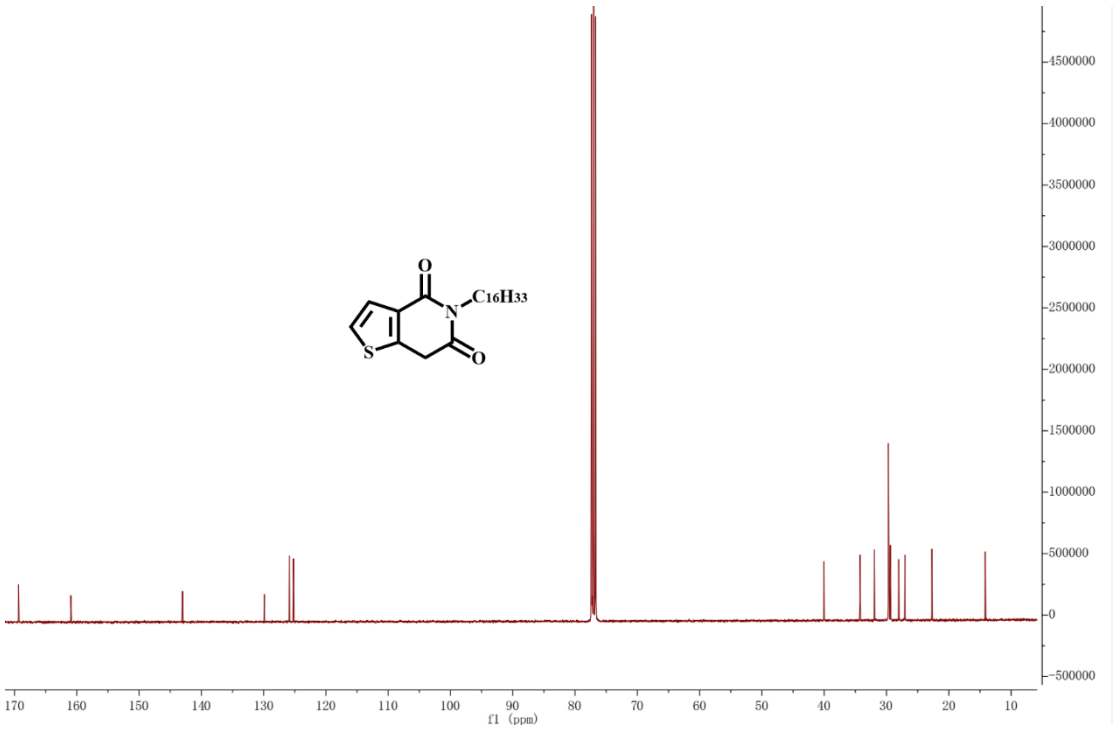

Figure S10. ^{13}C NMR spectrum of compound **2a**.

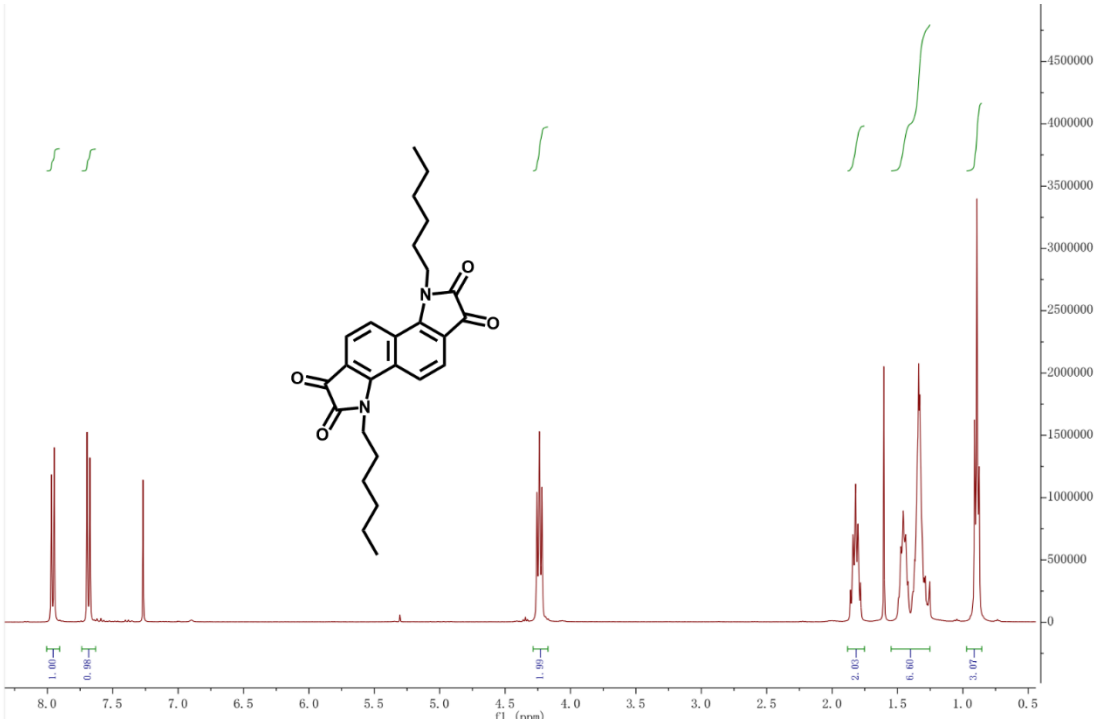

Figure S11. ^{1}H NMR spectrum of compound **4a**.

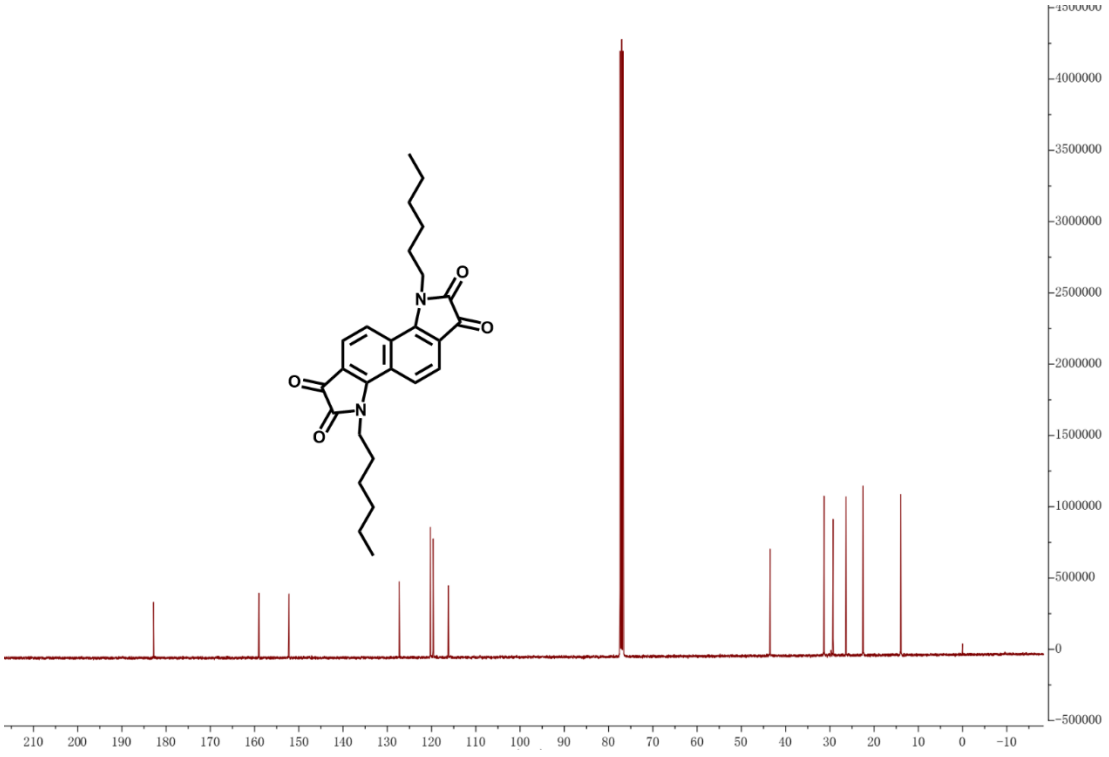

Figure S12. ^{13}C NMR spectrum of compound **4a**.

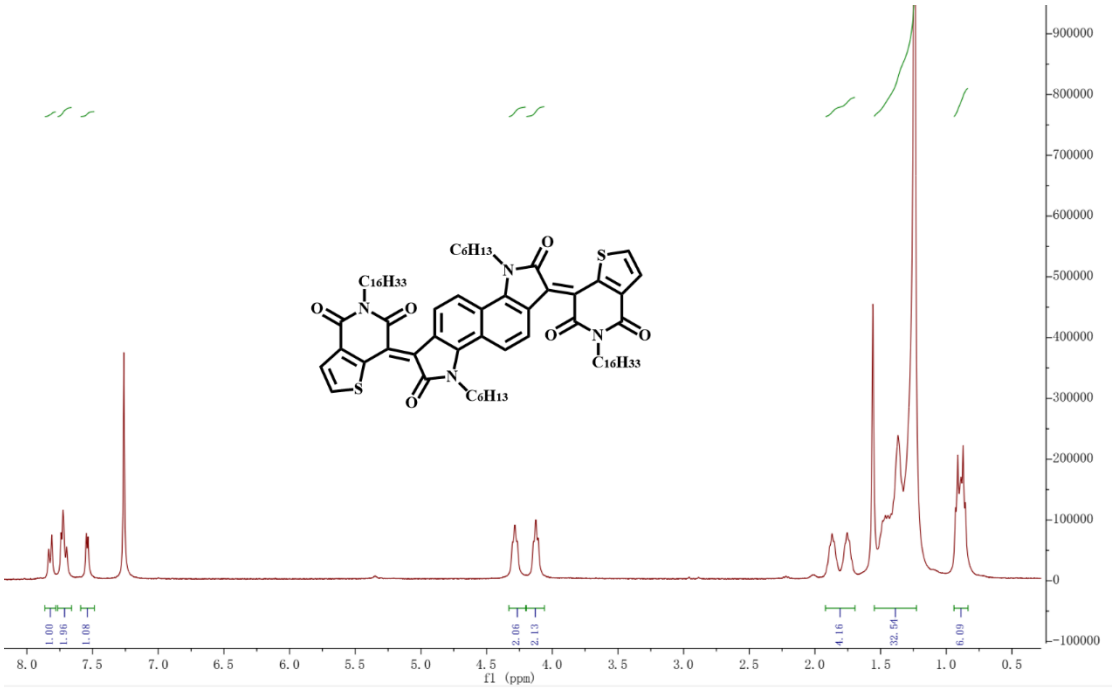

Figure S13. ^{1}H NMR spectrum of compound **TPBIID**.

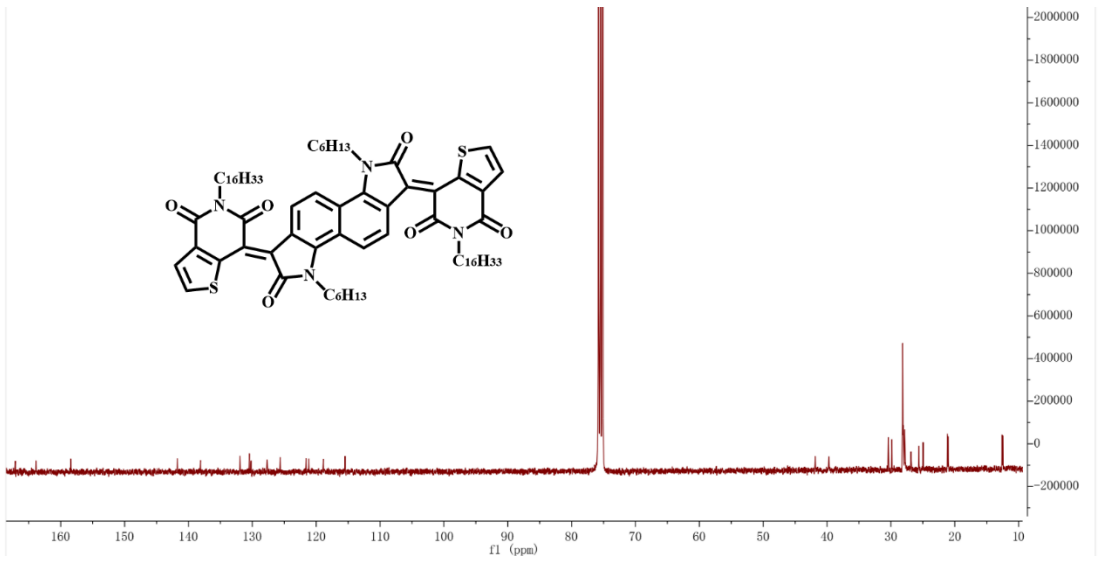

Figure S14. ^{13}C NMR spectrum of compound **TPBIID**.

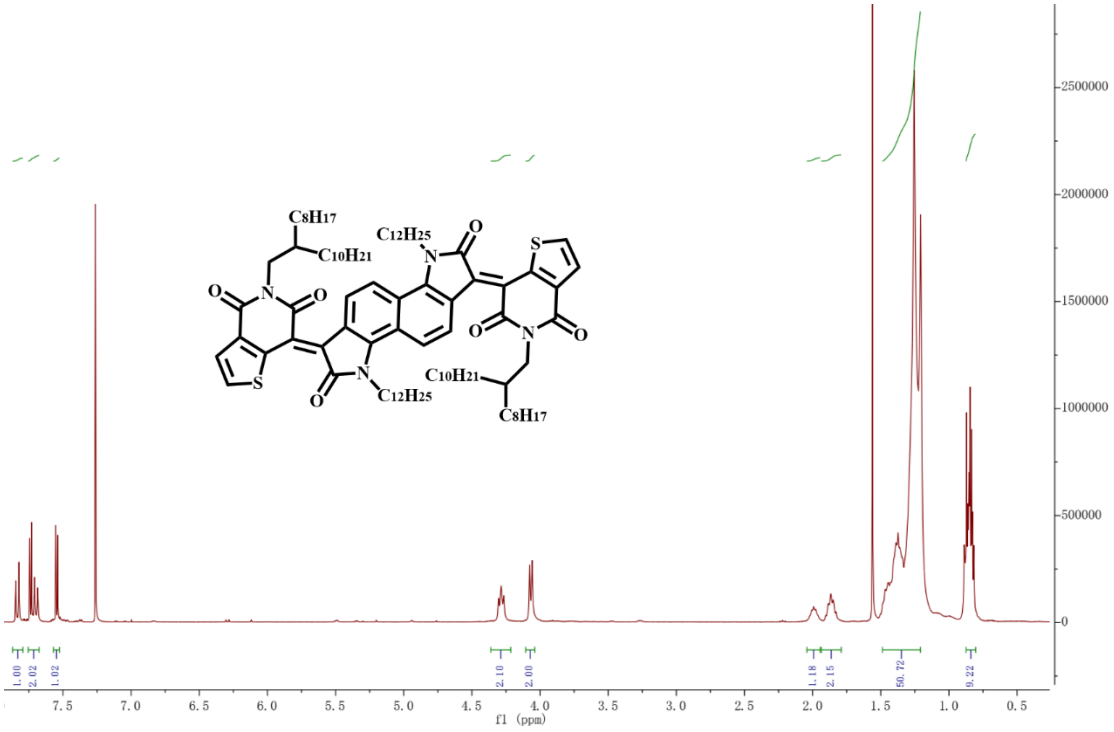

Figure S15. ^{1}H NMR spectrum of compound **TPBIID-OD**.

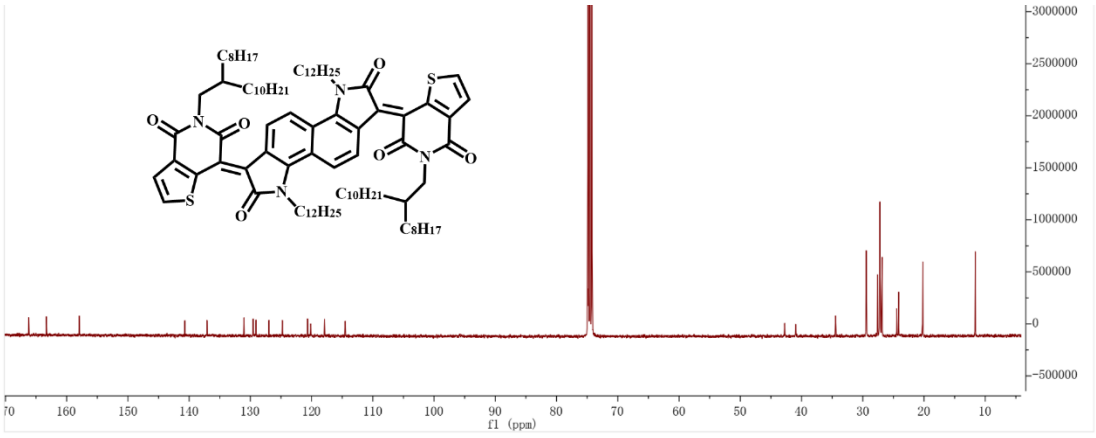

Figure S16. ^{13}C NMR spectrum of compound **TPBIID-OD**.

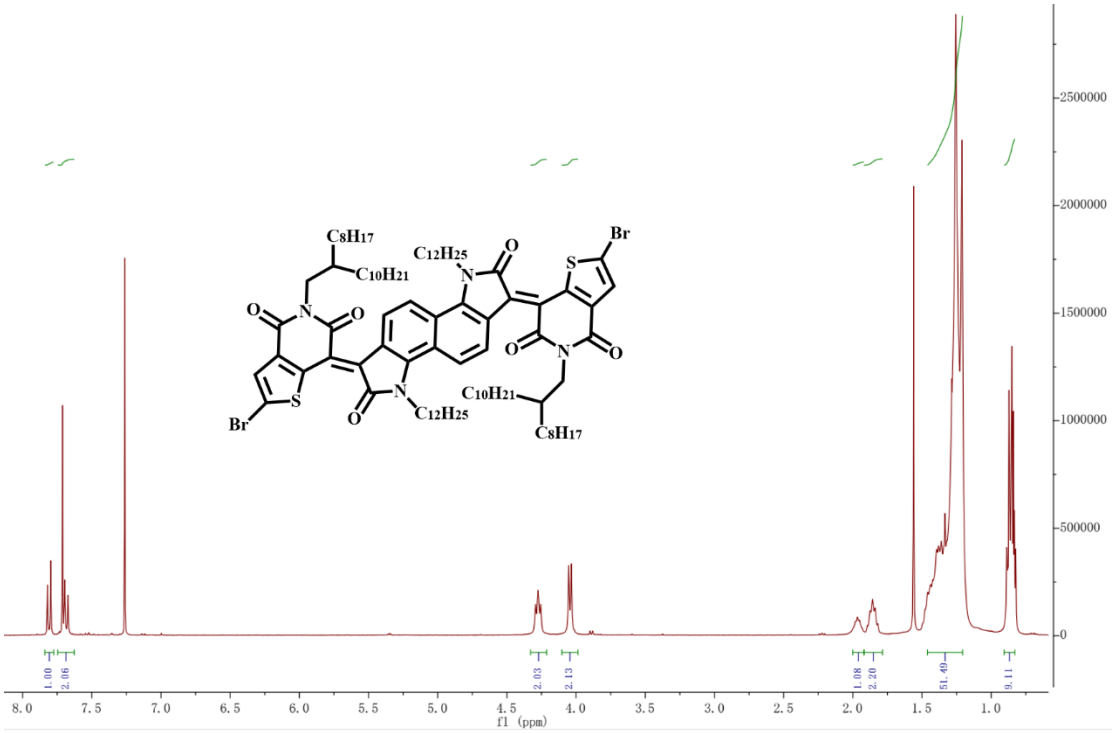

Figure S17. ^{1}H NMR spectrum of compound **5**.

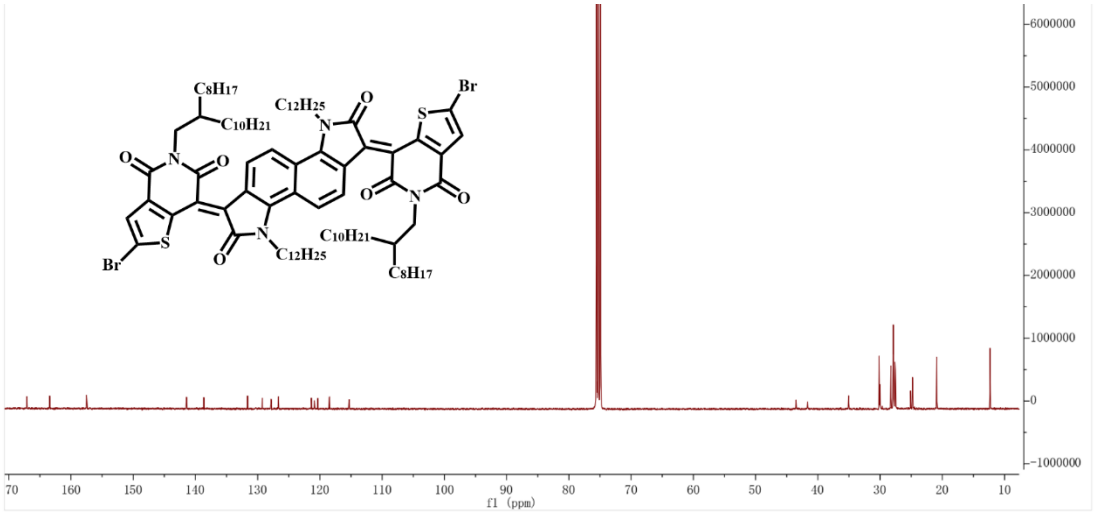

Figure S18. ^{13}C NMR spectrum of compound **5**.